REPORT DOCUMENTATION PAGE

Form Approved
OMB No. 0704-0188

1. REPORT DATE *(DD-MM-YYYY)*	2. REPORT TYPE	3. DATES COVERED *(From - To)*
08-12-2013	Final Report	05-15-2010 - 05-14-2013

4. TITLE AND SUBTITLE
Physical and Chemical Processes In Flames--Renewal 3-15-2009

5a. CONTRACT NUMBER
FA9550-10-1-0218

5b. GRANT NUMBER
FA9550-10-1-0218

5c. PROGRAM ELEMENT NUMBER

6. AUTHOR(S)
Law, Chung, K

5d. PROJECT NUMBER

5e. TASK NUMBER

5f. WORK UNIT NUMBER

7. PERFORMING ORGANIZATION NAME(S) AND ADDRESS(ES)
Princeton University
Mechanical and Aerospace Engineering Department
40 Olden Street, NJ-08544

8. PERFORMING ORGANIZATION REPORT NUMBER

9. SPONSORING / MONITORING AGENCY NAME(S) AND ADDRESS(ES)
Air Force Office of Scientific Research

10. SPONSOR/MONITOR'S ACRONYM(S)
AFOSR

11. SPONSOR/MONITOR'S REPORT NUMBER(S)

12. DISTRIBUTION / AVAILABILITY STATEMENT
No Restriction Distribution A - Approved for Public Release

13. SUPPLEMENTARY NOTES

14. ABSTRACT

The subject program, conducted through tight coupling between theory, experiment and computation and reported in 20 journal articles, has focused on the chemistry and dynamics of laminar and turbulent flames of surrogate jet fuels in environments simulating various operational aspects of aero-engines. For studies on combustion chemistry, we have experimentally acquired such chemistry-affected data as the ignition criteria and laminar flame speeds of fuel-air mixtures, which are respectively relevant for low- and high-temperature chemistries, and used these data to assist the development of their reaction mechanisms. For studies on flame dynamics, we have identified and classified various modes of intrinsic flame front instability for laminar flames, including thermal-diffusive cellular and pulsating instabilities, as well as the (cellular) hydrodynamic instability which is promoted at elevated pressures. For turbulent flames we have developed a novel apparatus allowing the study of expanding spherical flames in controlled turbulence and at constant, elevated pressures. The measured turbulent flame speeds show accelerative propagation and correlation with an appropriately-defined turbulent Reynolds number based on global flame radius and Markstein diffusivity.

15. SUBJECT TERMS

16. SECURITY CLASSIFICATION OF:			17. LIMITATION OF ABSTRACT	18. NUMBER OF PAGES	19a. NAME OF RESPONSIBLE PERSON
a. REPORT	b. ABSTRACT	c. THIS PAGE	UU	23	Chung K. Law
U	U	U			19b. TELEPHONE NUMBER *(include area code)* 609-258-5271

Standard Form 298 (Rev. 8-98)
Prescribed by ANSI Std. Z39.18

Report Type: Final Report

Primary Contact E-mail: cklaw@princeton.edu

Primary Contact Phone Number: 609-258-5271

Organization /Institution name: Princeton University

Award Information

Grant/Contract Title: PHYSICAL AND CHEMICAL PROCESSES IN FLAMES--RENEWAL 3-15-2009

Grant/Contract Number: FA9550-10-1-0218

Principal Investigator Name: Prof. Chung K. Law

Program Manager: Dr. Chiping Li

Report Information: Final Report

Reporting Period Start Date: May 15, 2010

Reporting Period End Date: May 14, 2013

Report Abstract

The subject program, conducted through tight coupling between theory, experiment and computation and reported in 20 journal articles, has focused on the chemistry and dynamics of laminar and turbulent flames of surrogate jet fuels in environments simulating various operational aspects of aero-engines. For studies on combustion chemistry, we have experimentally acquired such chemistry-affected data as the ignition criteria and laminar flame speeds of fuel-air mixtures, which are respectively relevant for low- and high-temperature chemistries, and used these data to assist the development of their reaction mechanisms. Auxiliary contributions include the formulation of a fitting formula for the falloff curves of unimolecular reactions, which is more accurate and easy to evaluate than the classical Troe formula, and the development of a Chemical Explosive Mode Analysis (CEMA) computation algorithm that allows on-the-fly assessment of the local reactivity of a mixture and thereby identification of the dominant modes of burning and flame stabilization dynamics.

For studies on flame dynamics, we have identified and classified various modes of intrinsic flame front instability for laminar flames, including thermal-diffusive cellular and pulsating instabilities, as well as the (cellular) hydrodynamic instability which is promoted at elevated pressures. The potential of self-turbulization through flame front wrinkling has also been assessed. For turbulent flames we have developed a novel apparatus allowing the study of expanding spherical flames in controlled turbulence and at constant, elevated pressures. The measured turbulent flame speeds show accelerative propagation and correlation with an appropriately-defined turbulent Reynolds number based on global flame radius and Markstein diffusivity.

Research Summary

PART I: DEVELOPMENT OF COMPREHENSIVE CHEMICAL KINETIC MECHANISMS FOR LARGE-SCALE COMPUTATIONS

1. Premixed and Non-premixed Ignition

The interest in the study of nonpremixed ignition of hydrocarbons is to understand the controlling mechanisms and responses of ignition in a strained flow field, in which chemistry and transport phenomena are inherently coupled. The parameters governing ignition not only are of practical interest but, together with those in other systems, such as shock tubes, flow reactors, well-stirred reactors and laminar flames, form an extensive matrix for the development and validation of comprehensive hydrocarbon oxidation mechanisms. In the past few years, we have been systematically and extensively acquiring experimental data and conducting computational simulation of the ignition of a number of fuels in the laminar counterflow, with pressure up to a few atmospheres. While the extent of fuel variation investigated is quite extensive, it is nevertheless still rather insufficient in that they are primarily gaseous under atmospheric conditions. To extend the investigation to fuels that are liquid under room conditions, a new experimental set up for the nonpremixed ignition in stagnation flow was designed for experimentation at elevated and reduced pressures, ranging from 0.61 to 3.0 *atm.*, and with quantified flow fields, respectively recognizing the importance of pressure on the ignition kinetics and the need to use the local strain rate to quantify the characteristic flow time. Measurement of the axial velocity profile was conducted with LDV over the local strain rates of 60 to 350/s. As in the counterflow ignition of gaseous hydrocarbons, the ignition temperature of *n*-heptane increases monotonically with increasing strain rate and decreasing system pressure.

Numerical simulation of the ignition response with detailed and reduced chemistry and transport was also conducted. The mole fraction of *n*-heptane at the liquid surface was found to be insensitive to the variations of strain rate and pressure examined in the present study, and its slight variation was considered to have minimal effect on the ignition response. A detailed high-temperature oxidation model,Mech-130, yielded better agreement with experiments than a smaller model, Mech-58, at 0.61 and 1 atmosphere, while the comparison is unclear at 1.5 and 3.0 atmospheres [*Fig. I-1*]. An explosive mode analysis was conducted using the kinetic mechanism of Mech-130 to facilitate understanding of the ignition mechanism. A transition from radical explosion to thermal explosion was clearly demonstrated by the explosion pointers [*Fig. I-2*]. An explosion participation index identified the controlling reactions leading to ignition. Reactions of the H_2/CO chemistry and those involved C_2-C_3 radicals were found to be important at the ignition states.

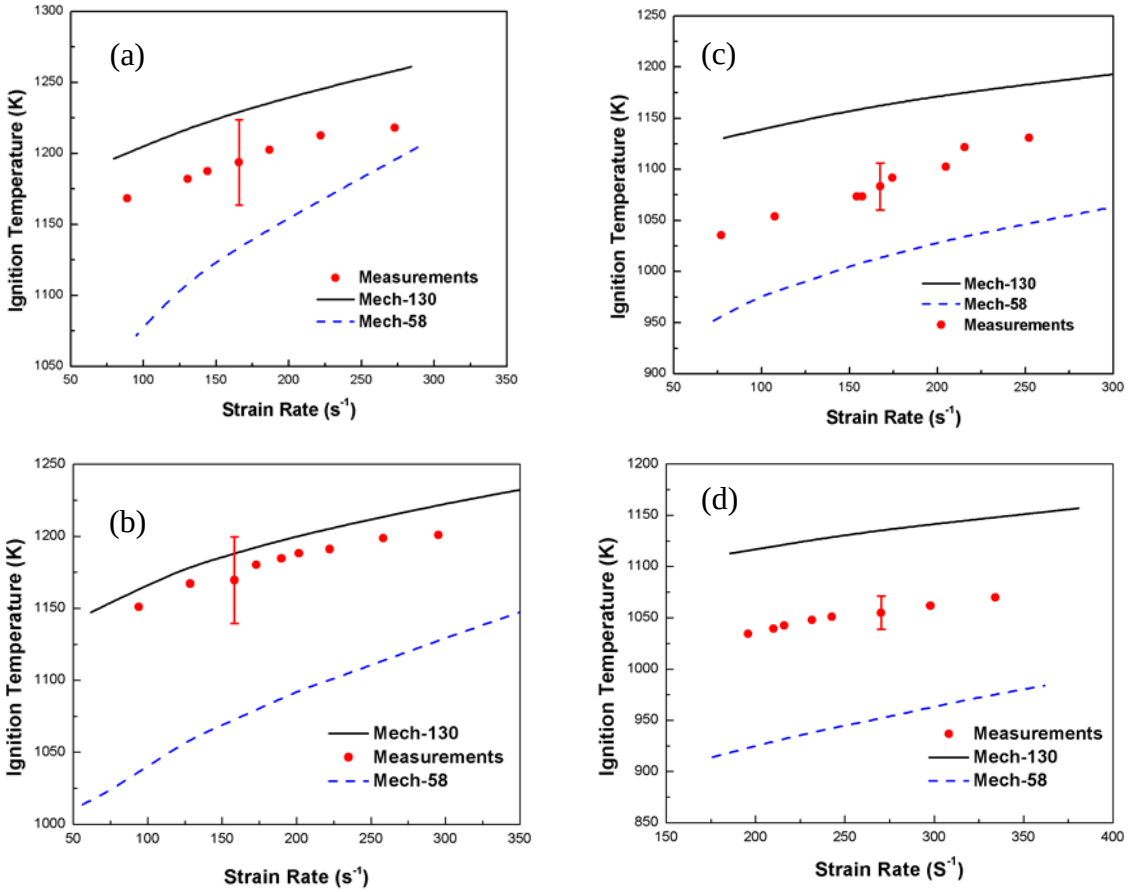

Figure II-1: (a) Measurement and simulation of ignition temperature versus strain rate; (a) p=0.61 atm, (b) 1.0 atm, (c) 1.5 atm and (d) 3 atm.

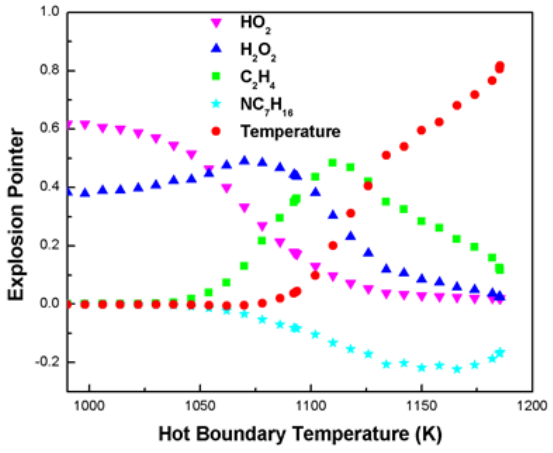

Figure I-2: Explosion pointer versus oxidizer temperature; p=1atm, $V_{boundary}$ =50 cm/s,

Following the work on *n*-heptane, we conducted a study to acquire experimental data on ignition temperatures in nonpremixed diffusive system and laminar flame speeds of $CH_4/C_2H_4/N_2$ mixtures. These data, together with numerical simulations using selected kinetic schemes, facilitate our understanding of the low- to intermediate-temperature ignition chemistry and high-temperature flame chemistry of ethylene-enriched methane, respectively. Computational analysis was then performed to identify the controlling elementary reactions in ignition and examine how the oxidation pathways shift with the relative fuel concentrations. Results show that ethylene addition enhances the ignitibility and flame propagation of methane. Furthermore, both the ignition temperature, T_{ign}, and the laminar flame speed respond steadily to variations of the ethylene concentration [*Fig. I-3*]. The experimental measurements were then compared with the simulation results to scrutinize the low- and high-temperature chemistry of the mechanisms, associated with ignition and flame speeds respectively. Results show that both mechanisms yield largely similar results for both the ignition temperature and laminar flame speed [*Fig. I-3*].

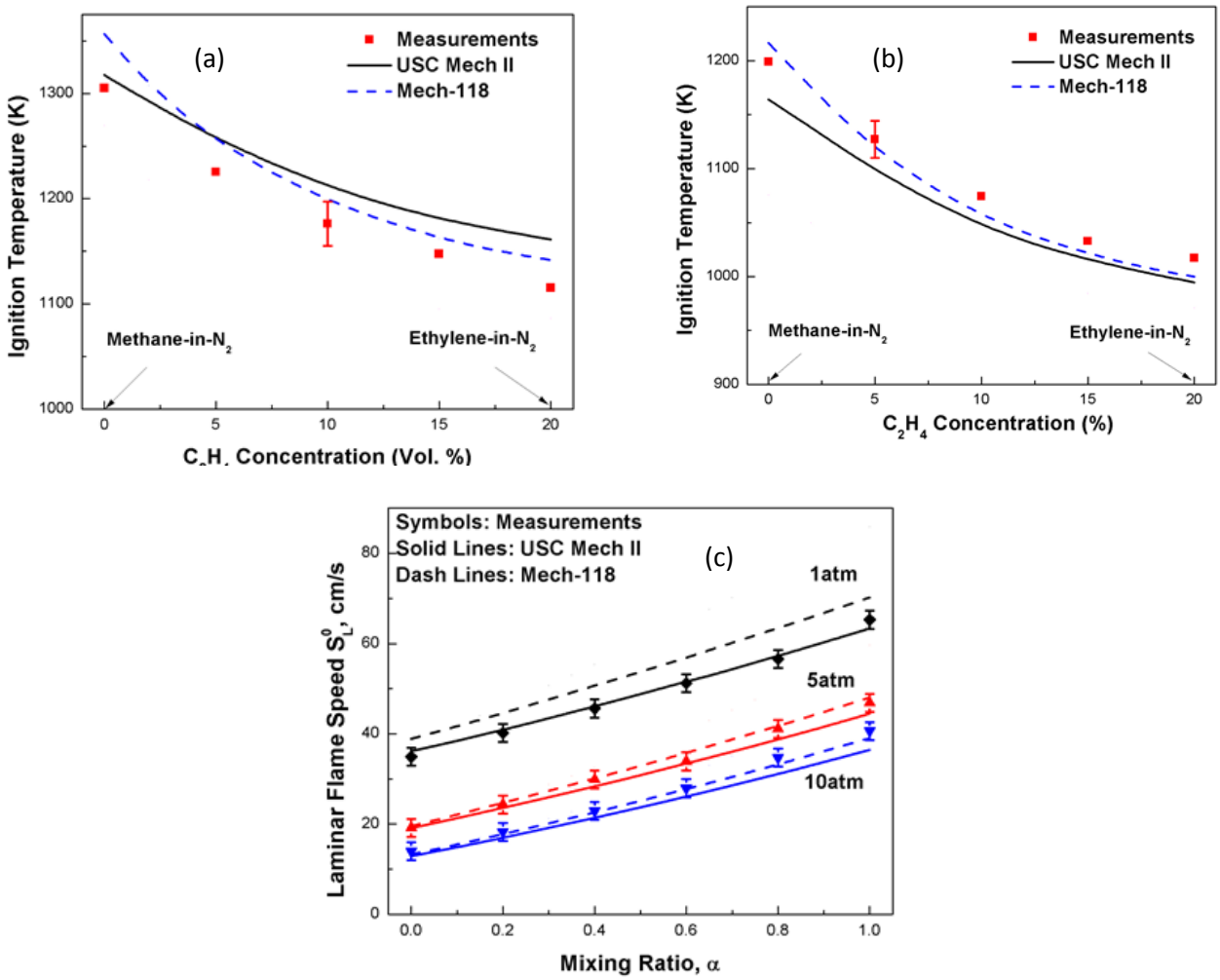

Figure I-3: Ignition temperature of CH_4/C_2H_4 mixture versus mole fractions of ethylene, (a) p=1atm, k=300/s. (b) p=5atm, k=300/s , (c) Laminar flame speeds of CH_4/C_2H_4 mixture versus mixing ratios at various system pressures, φ=1.0

The effects of thermal stratification (through both mean and fluctuations in initial temperature) and turbulent mixing timescales on the auto-ignition of a lean homogeneous *n*-heptane/air mixture at constant volume and high pressure were investigated by direct numerical simulations with a new 58-species reduced *n*-heptane/air kinetic mechanism. In the first parametric study, the homogeneous ignition delay was held constant, and twelve cases with varying initial mean temperature straddling the NTC regime were studied with different degrees of temperature fluctuations imposed. The displacement speed, Damköhler number, and chemical explosive mode analyses verify that, in general, larger *T'* induces greater temporal spreading of the mean heat release rate because the deflagration mode is predominant at the reaction fronts for large *T'*. However, spontaneous ignition prevails for small *T'*, and hence, simultaneous auto-ignition

occurs throughout the entire domain, resulting in an excessive rate of pressure rise. For mean temperatures lower than the NTC regime, e.g. with T_0 = 850 K, the ignition delay is increased with increasing *T'*. On the contrary, the ignition delay is significantly reduced with *T'* for mean temperatures greater than the NTC region (e.g. T_0 = 1008 K). For mean temperatures within the NTC region, e.g. with T_0 = 934 K, the combined effects of high and low temperatures manifest themselves such that the ignition delay is increased for small *T'* but is advanced with large *T'* [*Fig. I*-4]. In the second parametric study, the homogeneous ignition delays were halved and doubled for cases with T_0 = 1067 K and T_0 = 754 K, respectively. For the cases with high T_0 = 1067 K, the ignition delay is significantly reduced and the temporal spreading of the mean heat release rate is also enhanced with increasing *T'*, similar to the cases with T_0 = 1008 K. For cases with low T_0 = 754 K, however, the ignition delay and temporal spreading of the mean heat release rate are not significantly affected by thermal stratification. This is because the turbulence timescale (=2.49 ms) is short relative to the second-stage ignition delay time, and hence, thermal fluctuations are homogenized by fast mixing prior to the second-stage ignition. Therefore, the second-stage ignition is not significantly affected by turbulence.

Finally, in the third parametric study the ratio of the turbulence to ignition delay timescale was also found to change the ignition characteristics of the mixtures. A fast turbulence timescale is able to homogenize the mixture such that ignition is more apt to occur by spontaneous ignition for both large and small *T'* cases. Longer turbulence timescales, however, are not able to homogenize temperature fluctuations prior to thermal runaway. Therefore, for cases with small *T'*, ignition occurs independently in each ignition kernel, and for cases with large *T'*, ignition occurs primarily by deflagration, resulting in a smooth mean heat release rate. Overall, the effect of different turbulence timescales on the ignition delay is small compared with that of thermal stratification.

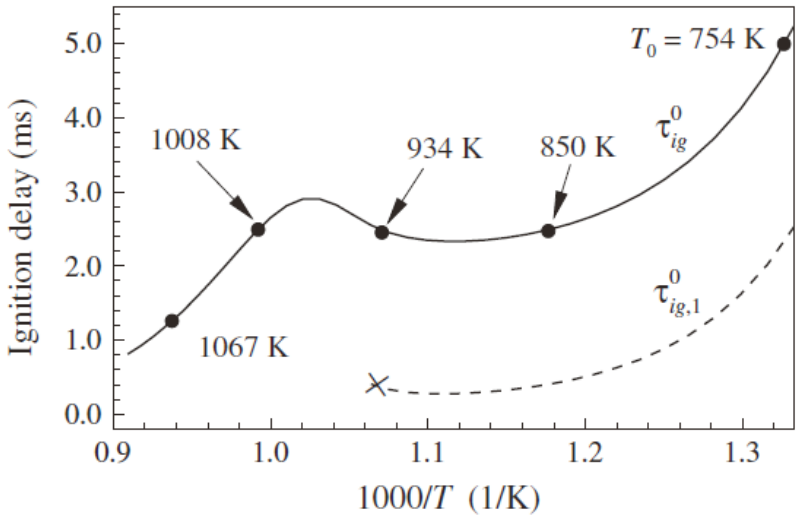

Figure II-4: Homogeneous ignition delay at constant volume with initial pressure of 40 atm as a function of initial temperature.

2. Studies on Chemical Kinetics

Unimolecular and the reverse recombination reactions play an important role in many chemical reaction systems related to atmospheric chemistry and combustion. Evaluation of these reaction rates is however computationally demanding because of their complicated pressure and temperature dependence, especially for large reaction systems. Approximate formulas of high accuracy are therefore desired in the simulation of these systems. Our recent work [*Zhang and Law (2009)*] approximated the fall-off curves of unimolecular reaction rate constants by proposing a fitting formula based on the Kassel integral, which is the unimolecular reaction rate expression of the classical RRK theory. Compared with previous formulas such as that of Troe [*Troe (1979), Gilber et al. (1983)*] and *Prezhdo (1995)*], this (ZL) formula not only is more accurate in the correlation, but it also has a simpler mathematical form that is computationally more efficient to evaluate. In this period of the project, we have extended the formulation by accounting for the effects of tunneling on unimolecular reaction rates and the corresponding falloff curves. A fitting formula for the pressure- and temperature-dependence of unimolecular reactions with tunneling is subsequently proposed. Compared to the Troe, Prezhdo and ZL formulas, the present formula shows substantially improved fitting precision in the tested reactions $C_2H_3 \rightarrow C_2H_2+H$, $C_2H_5 \rightarrow C_2H_4+H$ and i-$C_4H_3 \rightarrow C_4H_2+H$, for which tunneling becomes significant at different pressures and temperatures. As an improved version of the ZL formula, the present expression includes only one additional fitting parameter to describe tunneling. Furthermore, the tunneling correction factor also has a mathematically simple form for computational expediency.

During this period we have also focused on hydrogen abstraction reaction mechanisms. The hydrogen abstraction reaction of alkenes by the hydroxyl radical is dominant at temperatures above 700 K, because of the concomitant rapid reduction in the rate of the addition reaction due to fewer and less efficient stabilizing collisions of the adducts which tend to decompose thermally and rapidly before further reaction. The H-abstraction reactions of butene isomers by the OH radical were investigated by quantum mechanical and kinetics approaches. A comparative study of the geometry optimization and vibrational frequencies of the transition state structures of *s*-allylic H-abstraction was performed and it was found that results of the BHandHLYP/6-311G(d,p) method is comparable to those from the CCSD(T)/6-31G(d) method with efficient computational time. Consequently, the BHandHLYP/6-311G(d,p) method was applied to determine the electronic structures of the stationary points of the potential energy surface and the minimum-energy paths (MEP) of H-abstraction reactions of isomeric butenes by the OH radical. To increase the accuracy of the computed potential energy surfaces, single-point energy calculations were applied by using the CCSD(T)/6-311++G(d,p) method.

3. Flame Stabilization and Chemical Explosive Mode Analysis (CEMA)

Flame stabilization is essential in the understanding of lifted jet flames. Depending on the flame configuration, various stabilization mechanisms have been proposed based on premixed and non-premixed flames, auto-ignition, and turbulence–flame interactions. Some postulations involved are, however, difficult to verify with experiments, particularly when there is limited access to detailed spatial and temporal species information. Numerical simulation, particularly direct numerical simulation (DNS), provides abundant information associated with the complex flow and species fields. We have used DNS data for lifted turbulent jet flames set to extract the salient information on the controlling stabilization mechanism from the massive datasets.

We have developed the chemical explosive modes in chemically reacting flows, based on the concept of CSP, as a new diagnostic tool to delineate ignition and flame fronts in complex flows. An abrupt change in the mixture explosivity was employed for the detection of premixed flame fronts, which are difficult to detect using conventional methods involving only individual parameters such as temperature, mixture fraction, heat release rate and species concentrations.

A singular eigenvector matrix, or defective chemical Jacobian, was observed at the crossover point of the chemical explosive mode. It was found that this singularity was caused by the convergence of the explosive mode to the conservation modes. A species explosion index was consequently defined to normalize the diverging explosion pointers near the singularity. Radical explosion and thermal runaway were then distinguished with the explosion pointers for auto-ignition. The present method was first tested on homogeneous auto-ignition and one-dimensional laminar premixed flames and subsequently applied to analyze the DNS results of a turbulent lifted hydrogen jet flame in a heated coflow. Lean laminar and rich turbulent flame fronts were detected, and the bifurcation point preceding the two flame fronts was identified as the stabilization point. A Damköhler number based on the time scale of the explosive mode and the

scalar dissipation rate was defined to identify auto-igniting mixtures, and the role of auto-ignition as the mechanism for stabilization of the lifted flame was discussed.

PART II: DYNAMICS OF LAMINAR AND TURBULENT FLAME PROPAGATION

1. Flame Surface Instabilities

We have extended our previous work [*Jomaas et al. (2007)*] on the diffusional-thermal and hydrodynamic instabilities on spherically expanding stretched flames to include the study of spiral waves which originate from pulsating instabilities relevant for Le>1 mixtures such as the rich hydrogen-air and lean, C > 2, hydrocarbon-air mixtures [*Jomaas and Law (2010)*]. The experiments were conducted in our twin-chambered vessel that allows the spherical flame propagation at constant pressure. The experiment involved high-speed imaging at 2–25,000 frames/s. Five distinct unsteady phenomena were observed, namely, bulk oscillation, target patterns, ordered and disordered spiral waves, and extinction. Some of the key phenomena are shown in *Fig II-1*. We furthermore have experimentally mapped out the six flame responses in the phase space of pressure and equivalence ratio. In the order of appearance as the instability domain is approached, entered and traversed, we observed smooth flames, globally oscillating flames, flames with clear target patterns, flames with mixed patterns that are intermediate between targets and spirals, flames with clear spirals, and situations of no ignition. *Fig. II-2* shows this map for H_2-O_2 flames. Compared to H_2-Air flames we see a shift towards richer hydrogen concentrations. Given that the difference between Lewis numbers, *Le* is not expected to be significant for the two mixtures, one can infer that shift in the onset of the instabilities is caused by changes in the reactivity as represented by the Zel'dovich number, which is both directly and indirectly affected by the flame temperature. Another interesting observation of the H_2-O_2 flames is that flames at 40 and 60 atmospheres are actually stable at very rich conditions. In fact, stable flames are now found between flames with instabilities and flames that extinguish. This therefore demonstrates that the stability response can vary non-monotonically with increasing equivalence ratio, at high pressures. It is noteworthy that this observation was predicted and explained by *Christiansen et al. (2001)* who showed that the Sivashinsky stability parameter $Ze(Le-1)$ actually first increases and then decreases with increasing pressure for hydrogen-air flames. It order to evaluate the closeness of theoretical limit based on the Sivashinsky criterion with the experimental results we have evaluated the parameter $Ze(Le-1)$ as a function of the equivalence ratio for various pressures, where the values of *Ze* and *Le* were locally extracted from the response of unstretched and stretched flames respectively. *Fig.II-2* then superimposes the theoretical boundary on the plot of the experimental H_2-O_2 results, and it is seen that the experimental transition regime does span around the neighborhood of the theoretical boundary, suggesting: (1) the spiral flame is a phenomenon involving flame pulsation; (2) it is essential to use realistic, locally extracted thermokinetic parameters in evaluating the transition criterion.

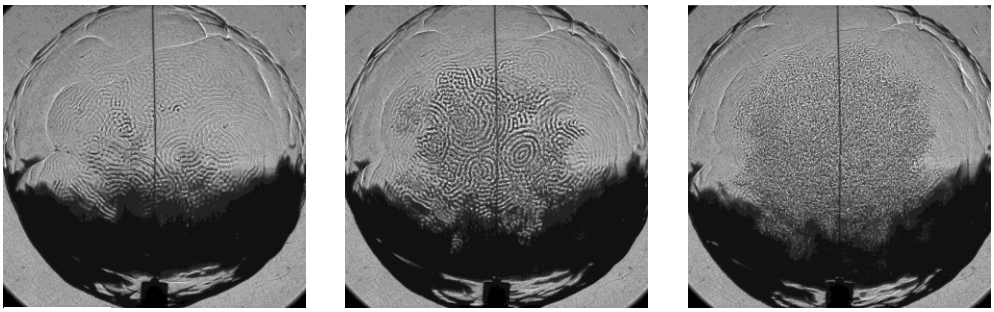

(a)

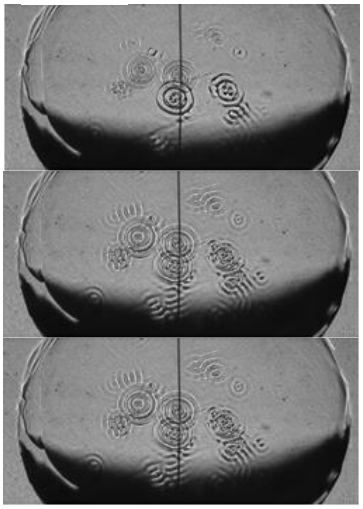

(b)

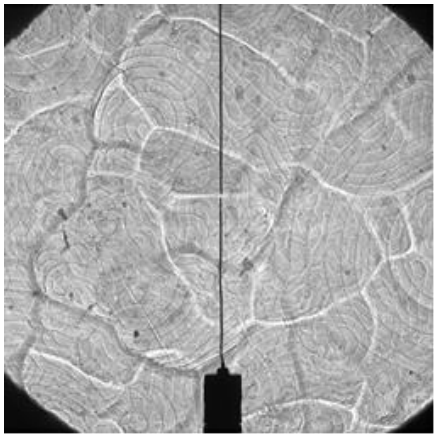

(c)

Figure II-1: (a) Target patterns on a spherically expanding lean butane-oxygen-helium flame (ϕ=0.59) at 30 atmospheres. The physical dimensions of the frames are 5.46cm by 5.46cm and the photographs were taken 0.625 ms apart

(b) Target patterns on a spherically expanding lean butane-oxygen-helium flame (ϕ=0.59) at 30 atmospheres. The frames are 2.73cm by 5.46cm and the sequence shows three consecutive frames at a framing rate of 15,000 fps. The global flame appears not to move in comparison with the rapid changes taking place on the flame front.

(c) A flame photograph of a hydrogen-air flame with an equivalence ratio of 4.30 at 20 atmospheres, showing the presence of spiral waves within the hydrodynamic cells. The

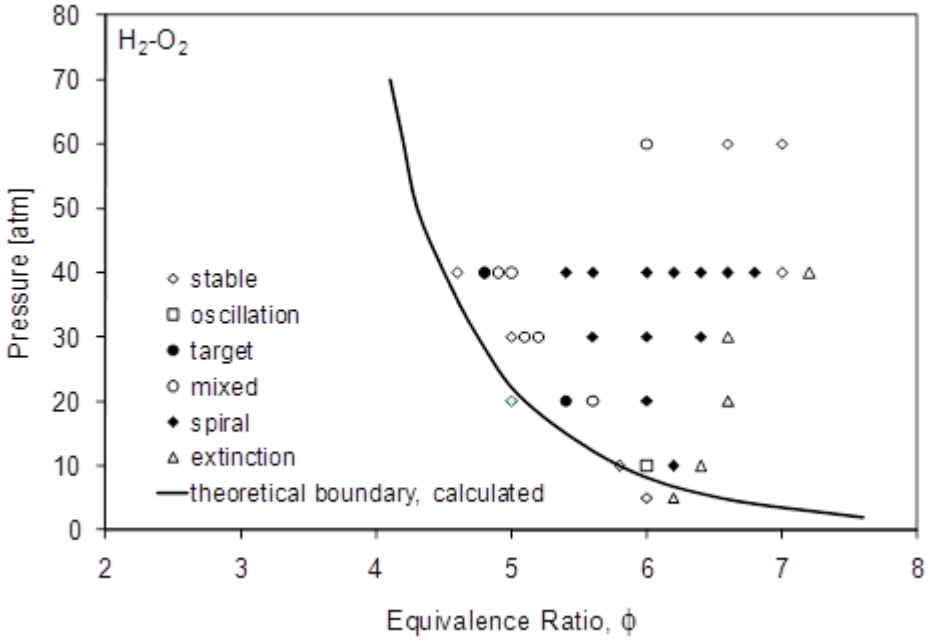

Figure II-2: Flame front mode diagram as a function of equivalence ratio and pressure for hydrogen–oxygen flames with the calculated theoretical boundary superimposed

An shown through many experiments, expanding laminar premixed flames is generally subjected to the excitation of flame front due to diffusional-thermal, hydrodynamic, and buoyancy induced instabilities, which are respectively caused by the non-equidiffusive nature of the diffusive scalars of species concentration and heat, the density jump across the flame, and body force in the presence of density gradient. The presence of cells over the flame surface increases its surface area and consequently also the global propagation speed of the flame. Furthermore, since new cells continuously evolve as the flame propagates, it is reasonable to expect that the flame speed will also continuously increase, leading to the possibility of self-acceleration. In order to quantify the flame acceleration due to constant evolution of cells and to assess the possibility of self-turbulization, we write the flame radius as a power function of time, $R_{av} \sim t^{\alpha}$, where α is a constant. Through experiments conducting in our dual chamber pressure vessel at high pressure such as 60 *atm*. with hydrogen flames, we achieve the required substantially smaller flame thickness that is suitable for studying cellular propagation [*Wu et al. (2013)*]. *Figs. II-3a and b* show that experiments with different ignition energies overlaps with each other and the slope of the $\log(U_{av})$ vs. $\log(R_{av})$ remains a constant until chamber confinement starts to have an influence, at about R_{av} = 2.0 cm. This result confirms that a self-similar regime does exist for wrinkled laminar flame propagation, after an initial transition period.

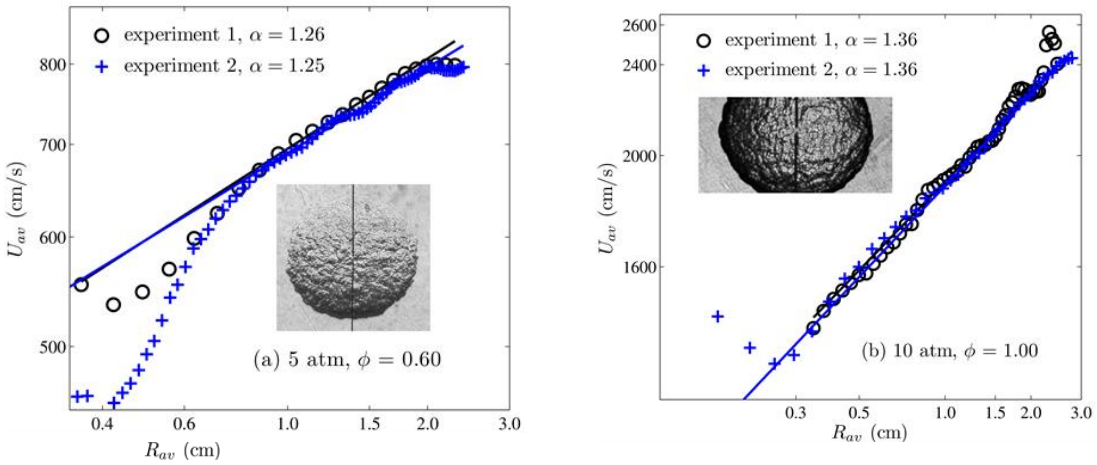

Figure II-3: Propagation velocity for two experiments for H2/air, at (a) 5 atm, ϕ= 0.60, and (b) 10 atm, ϕ = 1.00. Experiments 1 and 2 are runs with the same mixture but different ignition energies.

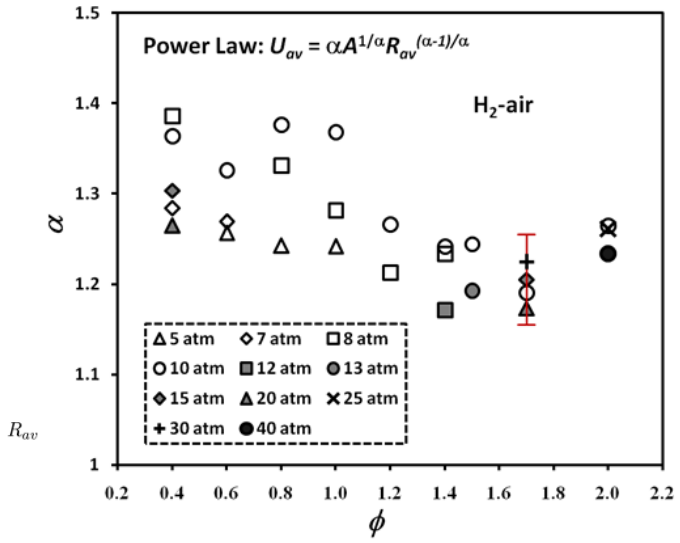

Figure II-4: Experimental acceleration exponents for H_2/air at various pressures and equivalence ratios (all data points are estimated to have uncertainty ±0.05; however, error bar is indicated only at one point for display clarity)

In *Fig. II*-4 we plot the experimentally measured acceleration exponent α for hydrogen/air mixtures as a function of the fuel equivalence ratio, φ, for various pressures. Three trends are observed. First, the values of α for lean mixture are higher than rich mixture due to the effect of diffusional-thermal instability, which is cellularly de-stabilizing for lean mixtures and stabilizing for rich mixtures leading to stronger and weaker wrinkling for these mixtures respectively. For

the strongly burning mixtures, with φ ranging from 0.60 to 1.20, we observe increasing pressure results in larger values of a, due to reduction in the flame thickness and thereby increase in the propensity of the flame to become hydrodynamically unstable. We also see that in the range of φ = 1.40 - 2.00, increasing the pressure does not change the value of α,

We also find that for hydrogen/air mixtures this is close to the stoichiometric value of φ= 1.00 (equidiffusive mixture), the acceleration exponent assumes a maximum value of about α = 1.37, is close to, but still sufficiently smaller than α = 3/2, the value purportedly related to the concept of self-turbulization.

2. Propagation of Turbulent Flames

The turbulent flame speed is a topic of wide interest in combustion and turbulence research due to its importance as a measure of flame surface density, in that it can be correlated to the volumetric heat release rate in a turbulent reacting flow. The problem is of considerable fundamental complexity, which is further compounded by the disagreement between theories as well as the high degree of scatter of the experimental turbulent flame speeds and their sensitivity on the geometry and type of the burner used in the investigation – a major hindrance that has prevented its utilization as a meaningful physical quantity for predictions and for validating simulations of turbulent reacting flows. In this research we seek a unified scaling description, at least under some special flow conditions such as those in homogenous isotropic turbulence. The most obvious choice of the flame parameters for such a scaling would be the planar laminar flame speed $S_L \sim \left(D\omega_b^0\right)^{0.5}$ and the corresponding laminar flame thickness $\delta_L \sim \left(D/\omega_b^0\right)^{0.5}$, assuming a local laminar flame structure exists, where D and ω_b^0 are the characteristic thermal diffusivity and reaction rate respectively [*Law 2006*]. The problem of turbulent flame propagation can then be considered as a geometric one in which the effect of turbulence is to wrinkle the flame at a multitude of length scales without perturbing the inner flame structure. Such a problem was considered analytically in [*Chaudhuri el al. (2011)*], which showed that for a statistically planar flame propagating in homogenous isotropic turbulence, the turbulent flame speed normalized by the corresponding laminar flame speed for large turbulent Reynolds number $\left(\mathrm{Re}_T\right)$ is given to the leading order by

$$S_T / S_L \sim \left\langle \sqrt{1+\nabla g \cdot \nabla g} \right\rangle \sim \left[1+\int_0^\infty k^2 \Gamma(k)\, dk \right]^{1/2} \sim \left[\left(u_{rms}/S_L\right)\left(\lambda_I/\delta_L\right) \right]^{1/2} \qquad \text{(II-1)}$$

where g is the fluctuating flame surface height/distance from the mean surface, k the wavenumber, $\Gamma(k)$ the flame surface spectrum obtained from spectral closure of the G-equation [*Peters (1992)*], u_{rms} the root mean square of velocity fluctuations and λ_I the velocity integral length scale which was assumed to be the flame hydrodynamic length scale.

Furthermore, in this research program we experimentally measured turbulent flame speeds in constant-pressure expanding flames, propagating in nearly homogenous isotropic turbulence. Utilizing the self-similar property of turbulent flame speeds evolving from the theory and experimental data presented, we showed that the turbulent flame speeds measured from the present spherically expanding flames, as well as those from literature data on Bunsen flames, can be scaled by a single parameter: a turbulent Reynolds number based on the geometric and transport properties of the flame. A configurationally independent description of turbulent flame propagation in near homogenous isotropic turbulence is thus proposed. Experimentally, we studied the flame propagation under different turbulence intensities for mixtures with Lewis Number close to unity at various pressures. Unlike laminar flames, turbulent flames are not symmetric in nature, thus the meaningful scale is given by mean radius $\langle R \rangle = \sqrt{A/\pi}$, where A is the area under the flame edge detected by Schlieren images. We observe the flame to accelerate as it propagates and gets larger, showing that turbulent flame speed does not hold a linear relationship with the radius of the flame.

To correlate the measured turbulent flame speed with the imposed turbulence parameters, *Eqn. (II-1)* provides insight for self-similar propagation if λ_I is replaced with the relevant largest flame length scale, *i.e.* hydrodynamic length scale of flame surface fluctuations which should be a linear function of $2\pi\langle R \rangle$ or simply $\langle R \rangle$ itself. Consequently, in *Fig. II-5* we plot $d\langle R \rangle / dt$, obtained from the experimentally obtained $\langle R \rangle$, normalized by the laminar flame speed with respect to the burnt gas (S_L^b), as a function of $\left[\left(u_{rms}/S_L\right)\left(\langle R \rangle/\delta_L\right)\right]$, i.e. the RHS of Eqn. (II-1) with the integral length scale being replaced by $\langle R \rangle$. The superscript *b*, as in S_L^b implies flame properties with respect to the burnt gas, whereas absence of a superscript implies flame properties with respect to unburnt gas. Since the thermal diffusivity $D \sim S_L \delta_L$, the term $\left[\left(u_{rms}/S_L\right)\left(\langle R \rangle/\delta_L\right)\right] = \mathrm{Re}_{T,\langle R \rangle}$ represents a turbulent Reynolds number with $\langle R \rangle$ being the length scale and the thermal diffusivity replacing the kinematic viscosity. It is then observed from Fig. 2 that all the data from different conditions of turbulence intensity and pressure, and at each instant of the propagation event, collapse reasonably well on a $\mathrm{Re}_{T,\langle R \rangle}^{\alpha}$ curve, with the exponent $\alpha = 0.54$ obtained by nonlinear least-square fitting over the entire relevant data set. This result therefore substantiates the possible validity of the 1/2-power scaling, as suggested by the theory of [24]. More importantly, it suggests that expanding turbulent flame propagation is self similar, at least in the domain of interrogation, as evident from the relationship

$$\left(S_L^b\right)^{-1} d\langle R \rangle / dt = O(1)\left[\left(u_{rms}/S_L\right)\left(\langle R \rangle/\delta_L\right)\right]^{1/2} \qquad \text{(II-2)}$$

The 1/2-power of *Eqn. (II-2)* also indicates that the turbulent flame is accelerating. This is due to the fact that as the flame expands during propagation, its smallest wavenumber decreases resulting in a continuous increase in the integral of the $k^2\Gamma$ spectrum or the flame surface scalar dissipation spectrum.

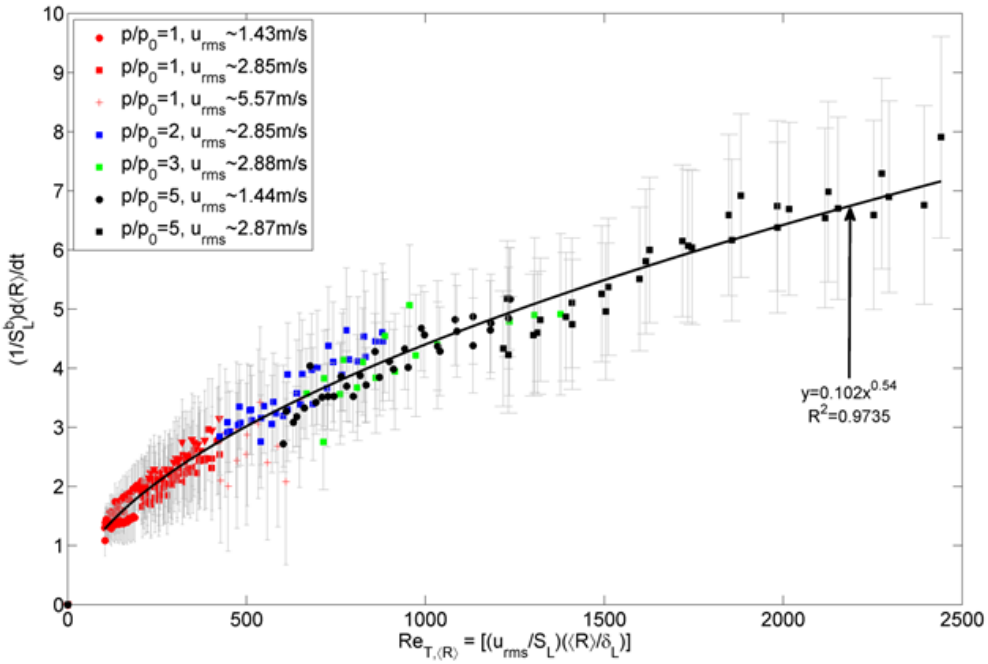

Figure II-5: Plot of flame propagation rate normalized by laminar burnt flame speed with respect to turbulent Re with average radius as length scale and thermal diffusivity as transport property. Not included in the fitting is the $p/p_0=1$, u_{rms}~5.57m/s *case as the Schlieren images show widespread local extinction in such flames and evident from their lower propagation rates.* u_{rms} *appearing in the abscissa is the* $u_{rms}(\langle R\rangle)$*, obtained by integrating over all* θ *.* u_{rms} ~ *denotes the average* u_{rms} *experienced by the flames during the propagation event. The error bars indicate the error that could be caused by the mean flow.*

Despite of the success of $\frac{S_T}{S_L}\sim\left[\frac{u_{rms}}{S_L}\frac{\langle R\rangle}{\delta_L}\right]^{1/2}$ on unity *Le* flames, it is widely recognized that *Le* of most mixtures can deviate substantially from unity to affect the flame temperature and subsequently the flame speed through the intrinsic Arrhenius kinetics. Therefore it is of interest to seek a scaling relation which takes into account the *Le* effects and is valid for all fuel/oxidizer mixture properties. The effect of non-unity *Le* in modifying the local flame speed is most prominent in the presence of local stretch and curvature due to the nonequidiffusion of heat and species which are directed normal to the local flame surface. The dependence of the local flame speed on strain and curvature is essentially nonlinear; however, it has been shown by *Chen*

(2011) and *Kelley et al. (2012)* for the outwardly expanding spherical flame, the empirical linear relation between local flame speed $\tilde{S}_L$ and curvature proposed by *Markstein (1951)* provides a reasonably accurate approximation, $\tilde{S}_L = S_L\left(1-\delta_M\kappa\right)$, where κ is the curvature with the convex section in the direction of flame propagation being positive, and δ_M is a coefficient having the unit of length and termed the Markstein length. The value of Markstein length in the unit of flame thickness is the Markstein number, $Mk = \delta_M/\delta_L$, which is a strong function of *Le.* For a turbulent premixed flame with positive Markstein length, the concave portion of the flame, with a negative curvature, propagates faster than the convex portion of the flame which has a positive curvature, leading to reduction of the surface fluctuations and thereby the total flame surface area. This *dissipative* mechanism is most amplified at large wavenumbers or large curvatures. By assuming that: (i) balance of Markstein dissipation by kinematic restoration and amplification by thermal expansion due to their similar wavenumber dependence (but with opposite signs) [*Peters et al. (2000)*]; (ii) the dominant role of dissipation by Markstein diffusion at large wavenumbers and thereby retaining Markstein diffusion as the sole dissipation mechanism; and (iii) turbulent flame speed is proportional to the total flame surface area, the following scaling relation (Eqn. (69) in [*Chaudhuri et al. (2011)*]) was arrived:

$$\frac{S_T}{S_L} \sim \left[\frac{1}{Mk}\frac{u_{rms}}{S_L}\frac{L_I}{\delta_L}\right]^{1/2} \sim \left[\frac{u_{rms}}{S_L}\frac{L_I}{\delta_M}\right]^{1/2} \qquad \text{(II-3)}$$

where L_I is the integral scale. With further consideration of hydrodynamic length scale for flame to be the brush thickness which scales with the mean radius of the flame, we arrive at

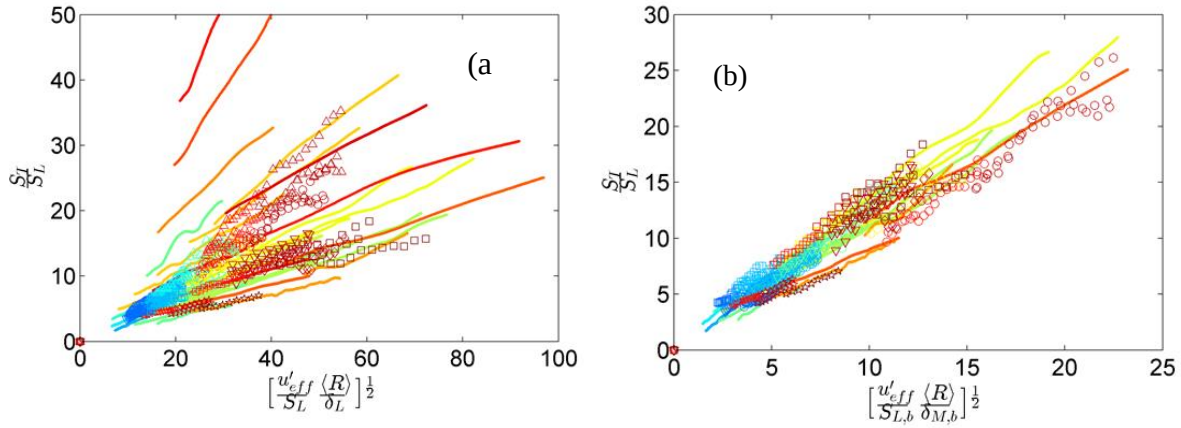

Figure II-6: Log-log plot of (a) $S_{T,c=0.5}/S_L$ versus $\sqrt{\left(u_{eff}^{'}/S_L\right)\left(\langle R\rangle/\delta_L\right)}=\mathrm{Re}_{T,f}^{0.5}$ and (b) $S_{T,c=0.5}/S_L$ versus $\sqrt{\left(u_{eff}^{'}/S_{L,b}\right)\left(\langle R\rangle/\delta_{M,b}\right)}=\mathrm{Re}_{T,M}^{0.5}$ for H_2/air, ϕ=4.0; CH_4/air ϕ=0.9; C_2H_4/air, ϕ=1.3; n-C_4H_{10}/air ϕ=0.8; and C_2H_6O/air ϕ=1.0 mixture from present experiments. The lines represent the iso-C_8H_{18} data from **Error! Reference source not found.**.

$$\frac{S_T}{S_L}\propto\left(\frac{u_{rms}}{S_L}\frac{\delta_T}{\delta_M}\right)^{\frac{1}{2}}\propto\left(\frac{u_{rms}}{S_L}\frac{\langle R\rangle}{\delta_M}\right)^{\frac{1}{2}} \qquad \text{(II-4)}$$

Figure II-6(a) shows $S_{T,c=0.5}/S_L$ vs. $\mathrm{Re}_{T,f}^{0.5}=\left[\left(u_{eff}^{'}/S_L\right)\left(\langle R\rangle/\delta_L\right)\right]^{0.5}$ for all the conditions in log-log plots. It clearly shows that the normalized flame speed has strong dependence on the Lewis number. *Figure II-6(b)* which plots $S_{T,c=0.5}/S_L$ vs. $\mathrm{Re}_{T,M}^{0.5}=\left[\left(u_{eff}^{'}/S_L\right)\left(\langle R\rangle/\delta_{M,b}\right)\right]^{0.5}$ shows collapse of the data on a single plot proving the utility of scaling as proposed in *Eq. II-4*.

3. Laminar Flame Speeds

We have investigated the laminar flame speed for a series of normal and cyclo-alkanes to build a database against which the chemical mechanism schemes can be validated. Using a newly developed apparatus that allows experimentation at elevated pressures and temperatures, the laminar flame speeds for *n*-pentane, *n*-hexane, *n*-heptane, and *n*-octane were measured at both atmospheric and elevated pressures [*Kelly et al. (2011a)*]. The resulting data [*Fig II*-7] show that these *n*-alkanes have similar flame speeds for a given equivalence ratio and pressure, and thereby

confirm the findings of *Davis and Law (1996, 1998, 1999)* while extending the result to elevated pressures. An examination of the computed flame structures for these fuels also shows similarity, hence substantiating the suggestion of *You et al. (2009)* on the nature of such a similarity. We have also demonstrated and explained that the influence of stretch decreases with increasing pressure because of the reduced flame thickness. This is an important result because it not only indicates that the systematic error associated with stretch effects in the determination of laminar flame speeds is reduced with increasing pressure, it could also simplify the modeling and understanding of turbulent flames in light of the diminished influence of stretch.

Furthermore, experimental data on the laminar flame speeds of iso-octane/air mixtures at atmospheric and elevated pressures were acquired using the counterflow flame and the outwardly expanding flame, while the non-premixed ignition temperatures were determined for an iso-octane pool in the stagnation flow of a heated air jet at atmospheric and slightly reduced/elevated pressures [*Kelly et al. (2011b)]*. These experimental measurements [*Fig. II-8*] were compared with calculations based on the mechanisms of *Curran et al.(2000)* and *Chaos et al.(2007)*, with the former mechanism systematically and substantially reduced, using directed relation graph and computational singular perturbation, to facilitate the calculation. It was found that the Curran mechanism yielded substantially higher laminar flames speeds as compared to the present experimental results while results from the Chaos mechanism agree well with the present measurements. These trends are in agreement with previous results on the laminar flame speeds for n-heptane. Both mechanisms yield acceptable comparison with the observed non-premixed stagnation ignition temperature.

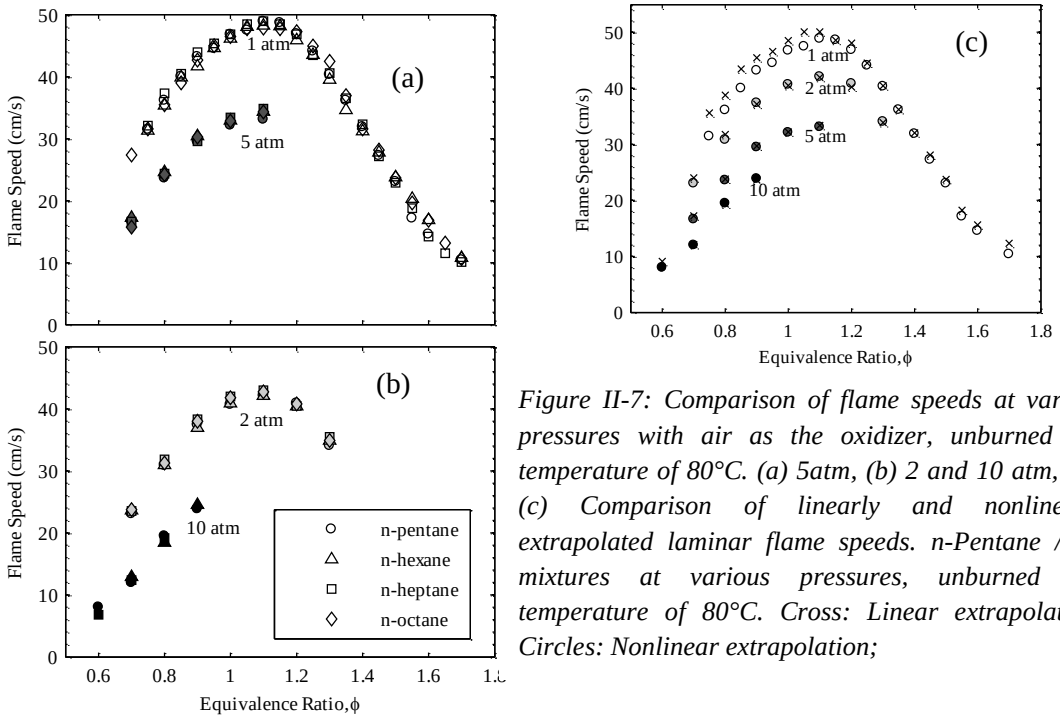

Figure II-7: Comparison of flame speeds at various pressures with air as the oxidizer, unburned gas temperature of 80°C. (a) 5atm, (b) 2 and 10 atm, and (c) Comparison of linearly and nonlinearly extrapolated laminar flame speeds. n-Pentane / air mixtures at various pressures, unburned gas temperature of 80°C. Cross: Linear extrapolation; Circles: Nonlinear extrapolation;

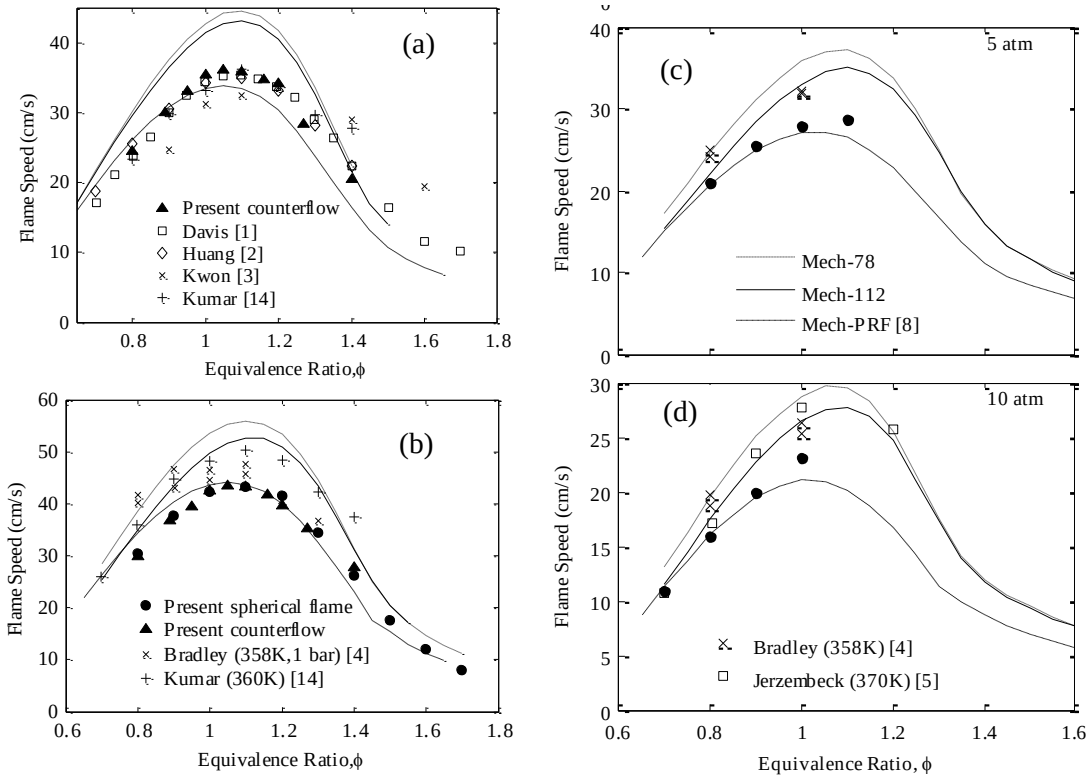

Figure II-8: Laminar flame speed of iso-octane / air, (a) 1 atm-298K, (b) 1atm-353K. Dashed-Line: Mech-PRF, Solid-Line: Mech-112, Dotted-Line: Mech-78, (c) 5 atm and (d) 10 atm.

References

A. P. Kelley, A. J. Smallbone, D. L Zhu, C. K. Law, *Proc. Combust. Inst.* 33, 963-970 (2011b)

A. P. Kelley, W. Liu, Y. X. Xin, A. J. Smallbone and C. K. Law, *Proc. Combust. Inst.* 33,501-508 (2011a).

C. K. Law, *Combustion Physics*, Cambridge University Press, NY (2006)

E. W. Christiansen, C. K. Law and C. J. Sung, *Combust. Flame* **124**, 35 (2001)

F Wu, G Jomaas and C K. Law, *Proceedings of the Combustion Institute*, Vol. 34, pp. 937-945 (2013)

G. H. Markstein, *Journal of Aeronautical Sciences* 18, 199, (1951)

G. Jomaas and C. K. Law, *Physics of Fluids*, 22, 124102 (2010).

G. Jomaas, C. K. Law, and J. K. Bechtold, J. Fluid Mech. **583**, 1, (2007)

H. J. Curran, P. Gaffuri, W. J. Pitz, C. K. Westbrook, *Combust. Flame* 129, 253–280 (2002)

J Troe, *J Phys Chem*, 83, 114–126 (1979)

M. Chaos, A. Kazakov, Z. Zhao, F. L. Dryer, *Int. J. Chem. Kinetics* 39, 399–414 (2007)

M. Lawes, M. P. Ormsby, C. G.W. Sheppard, R. Woolley, *Combust. Flame*, 159, 1949 (2012)

N Peters, *Journal of Fluid Mechanics*, 242, 611, (1992)

N. Peters, H. Wenzel, F. A. Williams, *Proc. Combust. Inst.* 28, 235 (2000)

O Prezhdo, *J Phys Chem*, 99, 8633–8637 (1995).

P. Zhang, C K Law, *Int J Chem Kinet*, 41, 727–734 (2009)

R G Gilbert, K. Luther, and J Troe, Ber Bunsen-Ges, *Phys Chem*, 87, 169–177 (1983)

S Chaudhuri, F Wu, D Zhu and C K. Law, *Physical Review E*, (2013) (in press)

S Chaudhuri, F Wu, D Zhu and C K. Law, *Physical Review Letters*, 108, 044503 (2012)

S Chaudhuri, V Akkerman and C K. Law, *Physical Review E*, 84, 026322 (2011)

S. G. Davis, C. K. Law, *Combust. Sci. Tech.* 140, 427–449 (1999)

S. G. Davis, C. K. Law, *Proc. Combust. Inst.* 26, 1025–1033 (1996)

S. G. Davis, C. K. Law, *Proc. Combust. Inst.* 27, 521–527 (1998)

V Akkerman, S Chaudhuri and C K. Law, *Physical Review E*, 87, 023008 (2013)

X. You, F. N. Egolfopoulos, H. Wang, *Proc. Combust. Inst.* 32, 403-410 (2009)

Z. Chen, *Combust. Flame*, 158, 291 (2011)

Archival Publications during Reporting Period

1. "Ignition of *n*-heptane pool by heated stagnating oxidizing flow," by W. Liu, D.L. Zhu, N. Wu and C.K. Law, *Combustion and Flame*, Vol. 157, pp. 259-266 (2010).

2. "Investigation on fuel-rich premixed flames of monocyclic aromatic hydrocarbons: Part 1. Intermediate identification and mass spectrometric analysis," by Y. Y. Li, L. D. Zhang, T. Yuan, K. W. Zhang, J. Z. Yang, B. Yang, F. Qi, and C. K. Law, *Combustion and Flame*, Vol. 157, pp. 143-154 (2010).

3. "Flame propagation and nonpremixed counterflow ignition of mixtures of methane and ethylene," by W. Liu, A.P. Kelley, and C.K. Law, *Combustion and Flame*, Vol. 157, pp. 1027-1036 (2010).

4. "Three-dimensional direct numerical simulation of turbulent lifted hydrogen/air jet flame in heated coflow: A chemical explosive mode analysis," by T. F. Lu, C. S. Yoo, J. H. Chen and C. K. Law, *Journal of Fluid Mechanics*, Vol. 652, pp. 45-64 (2010).

5. "Kinetics of hydrogen abstraction reactions of butene isomers by OH radical," by H. Y Sun and C. K. Law, *Journal of Physical Chemistry A*, Vol. 114, pp. 12088-12098 (2010).

6. "Observation and regime classification of pulsation patterns in expanding spherical flames," by G. Jomaas and C. K. Law, *Physics of Fluids*, Vol. 22, No. 12, 124102 (2010). **Selected as a research highlight of the journal; http://pof.aip.org/research_highlight_archive **

7. "Laminar flame speeds, nonpremixed stagnation ignition, and reduced mechanisms in the oxidation of *iso*-octane," by A. P. Kelley, W. Liu, Y. X. Xin, A. J. Smallbone and C. K. Law, *Proceedings of Combustion Institute*, Vol. 33, pp. 501-508 (2011).

8. "Laminar flame speeds of C_5 to C_8 *n*-alkanes at elevated pressures: experimental determination, fuel similarity, and stretch sensitivity," A. P. Kelley, A. J. Smallbone, D. L Zhu, C. K. Law, *Proceedings of Combustion Institute*, Vol. 33, pp. 963-970 (2011).

9. "A fitting formula for the falloff curves of unimolecular reactions: II. Tunneling effects," P. Zhang and C. K. Law, *International Journal of Chemical Kinetics*, Vol. 43, pp. 31-42 (2011).

10. "Direct numerical simulation of ignition of a lean n-heptane/air mixture with temperature inhomogeneities at constant volume: parametric study," C .S. Yoo, T. F. Lu, J. H. Chen, and C. K. Law, *Combustion and Flame*, Vol. 158. pp. 1727–1741 (2011).

11. "Measurements and correlation of laminar flame speeds of CO and C2-hydrocarbons with hydrogen addition at atmospheric and elevated pressures," by F. J. Wu, A. P. Kelley, C. L. Tang, D. L. Zhu and C. K. Law, *International Journal of Hydrogen Energy*, Vol. 36, No. 20, pp. 13171-13180 (2011).

12. "Spectral formulation of turbulent flame speed with consideration of hydrodynamic instability," by Swetaprovo Chaudhuri, V'yacheslav Akkerman and Chung K. Law, *Physical Review E*, Vol. 84, 026322 (2011).

13. "Fuel options for next generation chemical propulsion," by C. K. Law, *AIAA Journal*, Vol. 50, No. 1, pp. 19-36 (2012).

14. "Chemical explosive mode analysis for a turbulent lifted ethylene jet flame in highly-heated co-flow," by Z. Y. Luo, C. S. Yoo, E. S. Richardson, J. H. Chen, C. K. Law, and T. F. Lu, *Combustion and Flame*, Vol.159, pp. 265-294 (2012).

15. "Premixed flame propagation in a confining vessel with weak pressure rise," by A. P. Kelley, J. K. Bechtold and C. K. Law, *Journal of Fluid Mechanics*, Vol. 691, pp. 26-51 (2012).

16. "Laminar flame speeds of cyclohexane and mono-alkylated cyclohexanes at elevated pressures," by Fujia Wu, Andrew P. Kelley and Chung K. Law, *Combustion and Flame*, Vol. 159, pp. 1417-1425 (2012).

17. "Flame speed and self-similar propagation of expanding turbulent premixed flames," by Swetaprovo Chaudhuri, Fujia Wu, Delin Zhu and Chung K. Law, *Physical Review Letters*, Vol. 108, 044503 (2012).

18. "Hierarchical and comparative kinetic modeling of laminar flame speeds of hydrocarbons and oxygenated fuels," by E. Ranzi, A. Frassoldati, R. Grana, A. Cuoci, T. Faravelli, A. P. Kelley and C. K. Law, *Progress in Energy and Combustion Science*, Vol. 38, pp. 468-501 (2012).

19. "An experimental investigation on self-acceleration of cellular spherical flames," by Fujia Wu, Grunde Jomaas and Chung K. Law, *Proceedings of the Combustion Institute*, Vol. 34, pp. 937-945 (2013).

20. "Accelerative propagation and explosion triggering by expanding turbulent premixed flames," by V'yacheslav Akkerman, Swetaprovo Chaudhuri and Chung K. Law, *Physical Review E*, Vol. 87(2), 023008 (2013).

Changes in research objectives (if any): NA

Additional Information: NA

Change in AFOSR Program Manager, if any: Dr. Chiping Li is the new program manager succeeding Dr. Julian M. Tishkoff

Extensions granted or milestones slipped, if any: NA